


Magnetically Assisted Robotic Fetal Surgery for the Treatment of Spina Bifida

Journal Article**Author(s):**

Gervasoni, Simone; Lussi, Jonas; Viviani, Silvia; [Boehler, Quentin](#) ; Ochsenbein, Nicole; Moehrlen, Ueli; [Nelson, Bradley](#) 

Publication date:

2022-02

Permanent link:

<https://doi.org/10.3929/ethz-b-000531109>

Rights / license:

[In Copyright - Non-Commercial Use Permitted](#)

Originally published in:

IEEE Transactions on Medical Robotics and Bionics 4(1), <https://doi.org/10.1109/tmrb.2022.3146351>

Funding acknowledgement:

743217 - Soft Micro Robotics (EC)

180861 - A Submillimeter Minimally Invasive System for Cardiac Arrhythmia Ablations (SNF)

952152 - MAgnetically steerable wireless Nanodevices for the tarGeted delivery of therapeutic agents in any vascular rEgion of the body (EC)

Magnetically Assisted Robotic Fetal Surgery for the Treatment of Spina Bifida

Simone Gervasoni^{1*}, Jonas Lussi^{1*}, Silvia Viviani¹, Quentin Boehler¹, Nicole Ochsenbein^{2,4,5}, Ueli Moehrlen^{3,4,5†}, Bradley J. Nelson^{1†}

Abstract—Spina bifida is a congenital defect that occurs on the vertebral spine of a fetus. The most severe form causes exposure of the spinal cord and spinal nerve and has important repercussions on the life of the newborn child. Current prenatal operative procedures require laparotomy of the abdomen as well as hysterotomy of the uterus, which can result in severe consequences and risks for the mother. Here, we propose a robotically assisted endoscopic procedure based on magnetically steerable catheters to treat spina bifida defects in a minimally invasive way. The procedure can be performed in a fully remote manner using magnetic guidance and a haptic controller. Four custom magnetic catheter designs are presented to image, sever, grasp and close the lesion on the fetus back. We demonstrate our approach *in vitro* using phantom models of the abdomen, the uterus, and the defected fetus.

Index Terms—fetal surgery, magnetic navigation system, medical robotics, spina bifida, myelomeningocele.

Spina bifida is one of the most common neural tube defects that occurs in fetuses. It is estimated that almost 1 in 1000 newborn children in the western world suffer from neural tube defects, and approximately 140 000 cases occur worldwide every year [1], [2]. Spina bifida is the result of non-neurological occurring at the end of the first gestational months in the lumbosacral area of the spinal cord. This leads to an open neural placode which is exposed to the amniotic fluid and direct mechanical stress of the neuronal tissue. These factors lead to acquired spinal cord damage during pregnancy. The most severe form is myelomeningoceles (MMC), where the spinal cord lies on a cystic sac filled with cerebrospinal fluid, and a non-cystic lesion called myeloschisis [3], [4].

Both postnatal and prenatal surgeries can be considered to treat spina bifida. Postnatal surgery must occur within 48 hours after birth to avoid infection [2], and children treated in this way have a 78% chance of surviving through the 17th year of life [5]. Unfortunately, these repairs often require lifelong supportive care and lead to neurological deficits, hydrocephalus, and Chiari II malformations [6], [7].

The severity of postnatal neurological side effects increases over the gestation period and reaches a maximum with postnatal repair [8], [9]. For this reason, *in utero* prenatal repair is

the preferred method for treating MMC [10]–[13] and usually results in less postnatal deficits [14]. When performed in open fetal surgery, the mother undergoes an initial laparotomy and hysterotomy. This can lead to maternal and fetal complications [15].

Minimally invasive approaches for the treatment of MMC have recently been considered beneficial for *in utero* operation, drastically reducing the risks associated with the laparotomy and open hysterotomy [16]–[19]. While open hysterotomy and laparotomy can offer a higher degree of dexterity, we believe that the risks associated with these invasive procedures outweigh their benefits for the patient. For that reason a minimally invasive approach is preferred in this work. A manual minimally invasive approach consists of placing trocars on the mother’s abdomen to access the uterus and insert laparoscopic tools. The disadvantages associated with this approach include the use of long and rigid tools and a limited field of view compromising the fetal repair. [20].

To obtain the benefits of a minimally invasive approach and combat the disadvantages of the manual laparoscopic procedure, we propose for the first time a robotically assisted approach to treat MMC (Fig. 1). Our proposal is based on an endoscopic procedure using magnetically steered catheters. Magnetically steered catheters are highly flexible tools that allow significant bending to reach difficult areas inside the uterus, as opposed to straight and rigid conventional laparoscopic tools. Magnetic tools also increase the safety of the procedure as their flexible nature avoids damage to the mother or the fetus in case of contact. Magnetic fields are inherently bio-compatible with the human body, and allow for remote control of the tools. The dexterity offered by the magnetic navigation also allows for a decrease in the catheter diameter with respect to conventional tools [21]–[23]. This reduction in diameter and the improved steering dexterity lead to a reduction in the number and size of ports necessary for the magnetically guided procedure, further reducing the impact of the procedure on the mother [20].

In this paper, we demonstrate for the first time the use of magnetically controlled catheters for the treatment of spina bifida. We introduce four novel flexible magnetic catheters designed to fit within standard 11 Fr-trocars, and that can be steered magnetically to perform the procedure remotely and in a minimally invasive way. In section I we introduce our approach, the design of the custom magnetic catheters, and our magnetic navigation platform. In section II we demonstrate the use of the platform to perform the treatment of spina bifida *in vitro* using phantom models of the abdomen, the

* Shared first author

† Shared last author

¹ Multi-Scale Robotics Lab, ETH Zurich, Zurich, Switzerland

² Department of Obstetrics, University Hospital of Zurich, Zurich, Switzerland

³ Department of Pediatric Surgery, University Children’s Hospital Zurich, Zurich, Switzerland

⁴ The Zurich Center for Fetal Diagnosis and Therapy, University of Zurich, Zurich, Switzerland

⁵ University of Zurich, Zurich, Switzerland

uterus, and the defected fetus. These results are discussed in section III. Section IV concludes with an emphasis on the expected benefits of the proposed approach.

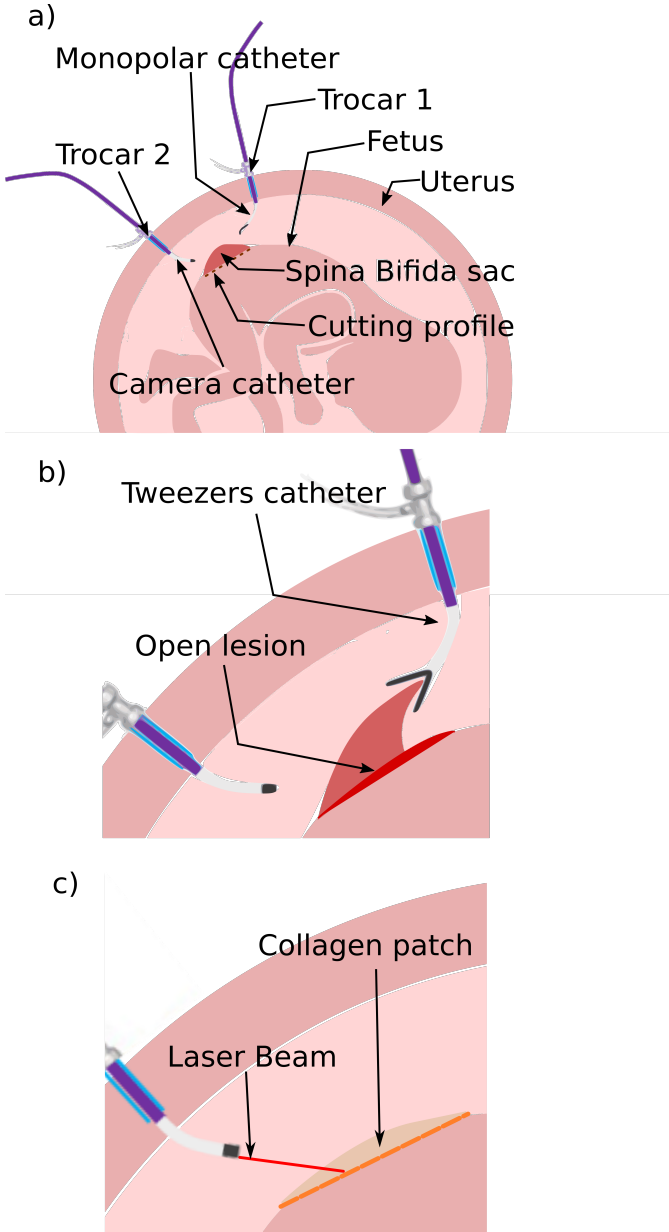


Fig. 1. Main steps for treating MMC using a magnetically assisted robotic approach. Two 11 Fr trocars are inserted through the abdomen into the uterus. First, a) the defect sac is cut with a monopolar catheter. The monopolar catheter is fed through one of the trocars. The other trocar is used to introduce the camera catheter. Then, b) a tweezers catheter is guided to peel off the cut spina bifida sac. The tweezers catheter is then retracted through the trocar using a mechanical catheter advancer (MCA). Finally, c) a collagen patch is unrolled to cover the open lesion and fixed in place using a surgical laser to locally melt the patch edge to the skin of the fetus.

I. MATERIALS AND METHODS

A. Proposed approach

A conventional *in utero* operation consists of a maternal laparotomy, hysterotomy and partial exteriorisation of the fetus's back and of the MMC lesion [16], [24]. Once the

lesion is exposed, it is separated from the surrounding skin, muscles, and meninges, and the MMC extra sac is resected. A neurosurgical multi-layer suture closure of the dura-mater, myofascial flap, and skin is then performed. The uterus and abdomen of the mother are finally closed by suturing. Babies who have undergone an *in utero* procedure for MMC are delivered by C-section during the 37th week of gestation.

The robotic procedure reproduces the three steps of this approach (Fig. 1a-c). It also dispenses with the laparotomy and hysterotomy associated with the open surgery [24]. Furthermore, it does not require multiple large laparoscopy ports [25] as only two 11 Fr trocars are used.

Suturing remains challenging using magnetic guidance, with only one example demonstrating this under magnetic steering [26]. The constraints of *in utero* procedures render their method impractical for our application. In our experimental settings, we adopted an alternative approach inspired by [27]–[29], where we simulated the future use of a personalised bio-engineered autologous skin-cartilage composite graft using a collagen patch to cover the back lesion [29]–[31]. To bond the patch to the skin of the fetus and seal the lesion, we followed the procedure demonstrated in [29], where the collagen patch edge is locally molten and bonded to the fetus skin using a laser.

Our magnetically guided assisted robotic procedure uses four custom magnetic tools remotely controlled by externally generated magnetic fields using an electromagnetic navigation system (eMNS). An eMNS consists of electromagnets located around the body of the patient, where the magnetic fields are modulated by the amount of electrical current that is running through their conductive windings [23]. To respond to the external magnetic field generated by the eMNS, the custom magnetic catheters are equipped with a set of permanent magnets along the flexible tip. Neodymium Iron Boron (NdFeB) permanent magnets at the tip allow the external magnetic fields to exert torque and bend the tip. The magnetic torque \mathbf{T} acting on a catheter's magnet is defined by the following:

$$\mathbf{T} = \mathbf{m} \times \mathbf{B} \quad (1)$$

where \mathbf{m} represents the magnetic dipole moment of the tip magnet, and \mathbf{B} is the magnetic field generated by the eMNS. The deflection of the catheter under the external magnetic field is determined by the relation between the stiffness of the catheter tip and the total magnetic dipole moment, which itself depends on the volume of the magnets, their position at the tip, and their magnetization [32], [33].

The magnetically assisted robotic procedure starts with the placement of two 11 Fr trocars on the abdomen of the mother to provide access ports to the uterus. The first trocar is used to insert custom magnetic tools to perform the surgery, and the second trocar is used to insert a camera catheter to provide an endoscopic view of the uterus. The procedure consists of three phases:

- 1) **Defect resection:** the sac around the defect is resected using a monopolar cutting tool mounted on a magnetic catheter. The catheter is guided along a close trajectory surrounding the defect sac (see Fig. 1a).

- 2) **Removal of the resected sac:** the resected sac is removed using tweezers, guided within a magnetic catheter, that are used to grasp the sac from the edge and carefully pull it away from the fetus. Once the sac is completely removed from the fetus' back, it is extracted through the trocar (see Fig. 1b).
- 3) **Covering the lesion:** the open lesion is covered using a collagen patch. A dedicated magnetic tool is used to deploy the collagen patch on top of the lesion to cover the exposed area. A laser is then used to locally melt the collagen patch to the fetal tissue creating a solid bond between the patch and the skin of the fetus (see Fig. 1c).

B. Custom magnetic catheters

1) *Monopolar magnetic catheter:* The first part of the procedure is performed using a magnetic catheter equipped with a monopolar cutting tip (see Fig. 2a and f). A monopolar cutting tool employs high frequency electric fields to cut and coagulate living tissues when the tip of the tools comes in proximity to, or has direct contact with, them. Monopolar cutting has the intrinsic advantage of immediately coagulating the performed cuts to avoid excessive bleeding. In addition, as it only requires contact with the tissue to perform a cut, it complements magnetically steered catheters as no force is required, as opposed to a traditional blade. The monopolar tip is integrated into an 11 Fr magnetic catheter. A copper cylinder is fixed at the catheter tip inside a set of custom cylindrical NdFeB magnets (sintered NdFeB N50H, X-Magnets, axially magnetized, China) as shown in Fig. 2a. The copper cylinder acts as an interface between the exchangeable monopolar tips and the catheter tip. The tip of the catheter contains three sets of cylindrical magnets separated by stainless steel springs. The assembly of magnets and springs is contained in a Pebax sleeve. The catheter tip is fixed to the main catheter body by overlapping a stiff Pebax 72D sleeve above the tip's soft Pebax 35D sleeve. The catheter body is internally supported by a long stainless steel spring. The stainless steel spring increases the buckling resistance of the catheter and allows for tighter bending radii.

The lumen of the catheter is formed by a polyamide tube through which a 0.3 mm diameter silver wire is inserted. The silver wire is laser-welded onto one side of the copper cylinder and on the other side to the connector of the electrosurgery generator unit used to actuate the monopolar cutting tool. A silver wire was chosen for its superior electrical conductivity and allows the use of a thinner wire compared to a traditional copper wire. The monopolar tips are inserted into the flexible copper cylinder and held in place by the friction between the tip and the copper cylinder.

2) *Tweezers magnetic catheter:* In order to remove the tissue cut from the fetus, we developed a catheter based on mechanically actuated tweezers combined with a variable stiffness (VS) section [34] (see Fig. 2b and g). The tweezers design is based on the interaction of the spring steel tweezers with the most distal cylinder magnet mounted in the catheter tip (see Fig. 2e). As demonstrated in [34], the tweezers are based on a Y-shaped spring steel structure consisting of a

Nitinol wire laser welded at the base of the tweezers. When the Nitinol wire is pulled with a force $F_{Nitinol}$, the shoulders of the tweezers interact with the edge of the cylindrical magnet forcing closure of the tweezers (see forces F_n and closure motion m Fig. 2e). A pulling force of 2 N on the wire is required to fully close the tweezers. Once the tension on the Nitinol wire is released, the tweezers reopen automatically under spring tension. The purpose of the VS tip is to make the catheter either flexible or rigid depending on the stage of the procedure. In order to navigate the tool safely using the magnetic field, the catheter is in its flexible state. When the tweezers need to be closed, the catheter changes to its rigid state in order to hold the tool in place while a pulling force is applied on the Nitinol wire. The ring magnet that interacts with the tweezers is fixed on the top of the VS module and enclosed in a Pebax sleeve. The VS module connects the tip with the ring magnet to the body of the catheter and is fixed to the body of the catheter using the outermost Pebax sleeve. The catheter body is supported by an internal stainless steel spring that provides rigidity and mechanical resistance to buckling of the body. The lumen is formed by a polyamide tube that runs through the entire catheter up to the ring magnets at the catheter tip. The Nitinol wire runs inside the polyamide tube.

3) *Patch magnetic catheter:* The patch catheter (see Fig. 2c) features a VS section and a magnetic tip with a 20 mm section of magnets. The tip contains solid cylindrical NdFeB magnets to supply the necessary force to deploy the patch. The patch is manually rolled over the Pebax tube of the tip before being inserted into the 11 Fr trocar.

4) *Camera magnetic catheter:* The camera catheter combines a camera (MD-T1001SLH-120-01, Misumi Electronic Corp.) with an additional lumen that is used to insert an optical fiber parallel to the camera module (see Fig. 2d and h). The camera and the lumen are encompassed by a set of magnets separated by stainless steel springs. The magnet-spring assembly is contained within a white Pebax sleeve constituting the tip assembly. The tip assembly is fixed to the catheter body via a rigid Pebax sleeve, and a stainless spring supports the rigid Pebax sleeve from the inside and offers buckling resistance when the catheter is pushed forward. The camera has an outer diameter of 2.5 mm and includes an LED illumination ring with variable intensity. The camera module has a resolution of 400×400 and a frame rate of 30 fps.

C. Electromagnetic navigation system

In this work we used a custom three-electromagnet eMNS called MagHead (see Fig. 3b). The MagHead enables the generation of magnetic fields up to 20 mT in magnitude in a $250 \times 250 \times 250$ mm open volume in front of its coils. The system is externally controlled using a control computer running Linux O.S. (Ubuntu 18.04), and a Robot Operating System (ROS) interface that communicates with the embedded computer of the eMNS via a TCP/IP protocol. The external computer converts the magnetic field target to the current targets using a calibrated magnetic model. The required current values are then sent via a TCP/IP protocol to the embedded computer.

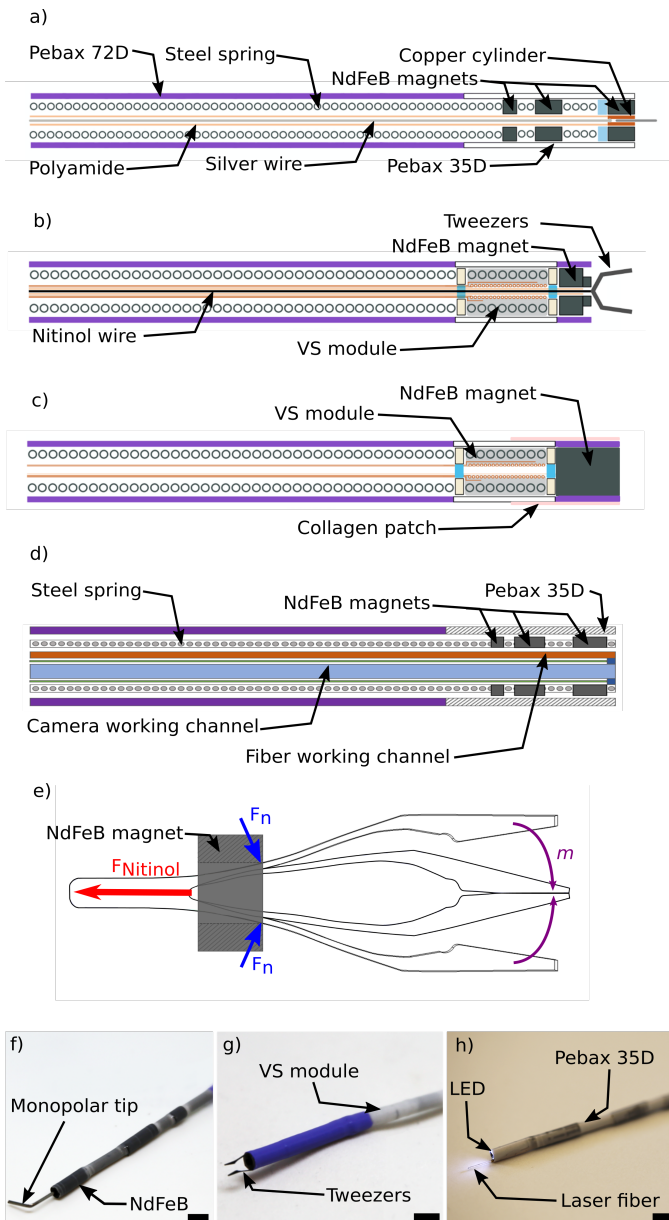


Fig. 2. Custom magnetic catheters. a) Monopolar catheter; the cutting tip of the catheter is connected to the electro-surgical unit via the silver wire. b) Tweezers catheter; the Nitinol wire is used to open and close the spring steel tweezers at the tip. c) Patch catheter with the porcine collagen patch wound around the tip. d) Camera catheter containing a camera, LED illumination and working channel with laser fiber. e) Mechanical actuation of the compliant tweezers. f) Monopolar catheter prototype with curved cutting monopolar tip (Scale bar 5 mm). g) Tweezers catheter with VS module in white (Scale bar 5 mm). h) Camera catheter with LED ring illumination and 500 μm optical fiber (Scale bar 5 mm).

D. Control interface

The control of the catheter direction is performed using a Phantom Omni haptic device. The Phantom Omni provides an absolute reference position through its control interface allowing for intuitive control of the magnetic catheter. The control of the catheter tip direction is carried out by orienting the Phantom Omni stylus in the direction the operator wants to point the catheter tip (see Fig. 3a). The system is calibrated such that the catheter axis is always parallel to the stylus axis.

As the orientation of the Phantom Omni's stylus corresponds to the orientation of the catheter's tip, the surgeon always has an external spatial reference for the direction in which the magnetic tool is pointing.

The surgical catheter is advanced using a mechanical catheter advancer (MCA). Two buttons located on the Phantom Omni stylus are used to advance and retract the catheter through the MCA.

The control computer is used to acquire the configuration of the input device and generate the target magnetic field accordingly. It also controls the MCA and the state of the VS element. The control computer provides feedback of the magnetic field direction and the position of the catheter with respect to the advancer. The intensity of the magnetic field as well as the speed for advancing and retracting the catheter through the trocar can be set using the interface.

E. Electrosurgical and laser units

An electro-surgical unit (Erbe ICC 350, Erbe Swiss AG) was used to control the monopolar cutting tool. The cutting function of the monopolar catheter is activated using a standard electro-surgical pen connected in series with the catheter.

The laser is activated using a pedal connected directly to a laser unit (KLM Nd:YAG-Laser MY 60) that is capable of delivering an 80 W laser beam through a 500 μm glass fiber. For the purposes of this study we used a power of 20 W.

F. Experimental setup

1) *Fetus and womb models*: To simulate the procedure *in vitro*, phantoms of the womb and the fetus were created. The 3d models used for this purpose were segmented manually from MRI data. The MRI data were taken at the 26th week of gestation and represent realistic conditions for a spina bifida operation. In the area of the defect, the fetus model was modified with a pocket and a path return electrode to accommodate the tissue simulating materials and allow the use of the monopolar catheter. The uterus was fixed to a model of a pregnant woman's abdomen. The fetus, uterus, and abdomen models were all 3d-printed using a polycarbonate FDM printer. A copper plate was glued onto the back pocket of the fetus to act as a counter electrode of the electro-surgical unit used for the monopolar cutting.

2) *Lesion simulation*: The cavity containing the counter electrode was filled using a tomato disk which provided an acidic environment to promote electric charge transmission with the counter electrode, in addition to providing visual color contrast feedback. The outermost layer was formed by a 1 mm-thick disk made of porcine flesh. Porcine flesh was chosen as it is readily available and closely emulates human flesh [35], [36]. The porcine flesh layer was placed on top of the tomato disk and set to be flush with the outer surface of the fetus model.

3) *Patch model*: We utilized a porcine collagen patch inspired by [29]. The porcine collagen patches on the patch catheter were cut from large square foils. The collagen patches were made flexible by moistening with water before rolling them onto the patch catheter tip.

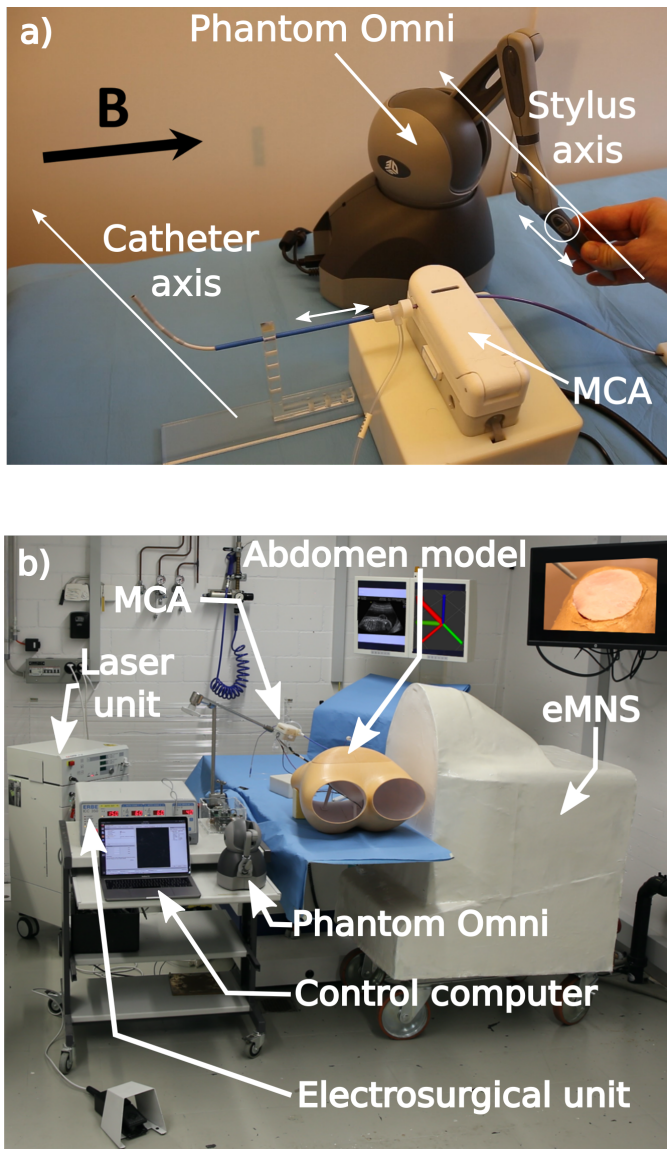


Fig. 3. Experimental setup. a) Phantom Omni, MCA and magnetic catheter. When the Phantom Omni stylus rotated around a specific axis, the catheter rotated at the same angle. Two buttons were used to advance and retract the catheter with a preset speed. b) Fetal surgery setup for the operation of MMC, the abdomen model containing the womb and fetus was placed on the surgical bed. The electromagnetic navigation system was placed on the right side of the patient and aligned with the fetus position. The magnetically guided catheter was inserted into the model via an 11 Fr catheter and fixed to the customized mechanical catheter advancer. The electrosurgical unit and the laser unit were on the opposite side of the surgical bed, ready to be connected to the respective magnetic catheters. The Phantom Omni and the control computer were placed near the model on a movable cart. A pedal control was used to fire the laser.

4) *Surgical setup*: The surgical setup used for *in vitro* testing is depicted in Fig. 3b. The abdomen was placed on a surgical bed, with the eMNS on the left side of the patient. The eMNS workspace center was aligned with the fetus to enable improved actuation of the magnetic tools. The electrosurgical unit and the laser were positioned on the other side of the surgical bed. The catheters were engaged in the MCA that was mounted on a surgical arm affixed to the bed rail. The trocars holding the magnetic catheter were mounted to the MCA using a removable bracket.

The magnetic tools were introduced using 11 Fr trocars puncturing through the abdomen and the uterus. Two trocars were used simultaneously, the first trocar carried the tool for the first two steps. This trocar was fixed to the MCA and was used to guide the monopolar catheter and the tweezers catheter. The second trocar carried the camera catheter throughout the three steps of the procedure. In the first two steps, the camera catheter was used for image feedback to guide the monopolar catheter, and the tweezers catheter was used to cut and remove the spina bifida sac. To prevent the camera catheter from moving under the external magnetic field during the first two steps, the camera catheter was advanced 10 mm past the end of the trocar. The flexible part of the camera catheter's tip remained inside the trocar's rigid sheath and prevented the camera from bending as the external field changed direction to guide the other tools. In the third step of the procedure, the camera catheter was used to provide visual feedback of the deployment of the porcine collagen patch, and the patch catheter was used as an active tool to laser the collagen patch to the fetus' skin.

II. RESULTS

A. Defect resection

The monopolar catheter was advanced in the uterus volume prior to the magnetic field being enabled. For the experimental defect resection, a field magnitude of 20 mT was used. This magnitude resulted in a stable catheter behavior for all directions. The electrosurgery unit was set to a cutting power of 150 W. The monopolar catheter was guided to the center of the porcine flash disk (Video S1 6s), a square flap with 10 mm-sides was cut from the center by steering the monopolar catheter in a square trajectory using the Phantom Omni (Video S1 19s). Sequences of an experimental resection are depicted in Fig. 5. After the cut was completed, the monopolar catheter was retracted using the MCA until the trocar seal was reached, the catheter was subsequently removed from the trocar by hand (Video S1 27s).

B. Removal of the resected sac

To remove the cut porcine flesh flap, the tweezers catheter was inserted into the trocar connected to the MCA. The tweezers catheter was manually pushed through the seal and engaged in the MCA. The tweezers catheter was advanced towards the cut flap using the MCA (Video S2 6s). When the catheter was above the porcine flesh flap, the VS section was transitioned to the flexible state via the control unit (Video S2 8s). The VS section takes approximately 6 s to transition from the stiff state to the flexible state. Once the variable section was flexible, the catheter tip was bent towards the flap. Tweezers were then used to grasp the flap from the edge (Video S2 18s).

When the tips of the tweezers reached the edge the porcine flesh flap, the VS section was transitioned back to its stiff state (Video S2 24s). The Nitinol wire was pulled using a manual handle fixed at the end of the catheter. The manual handle was locked in place to keep the tweezers closed. The action of the Nitinol wire closed the tweezers to grasp the flesh flap within the tips (Video S2 26s). A pulling force of approximately 2 N

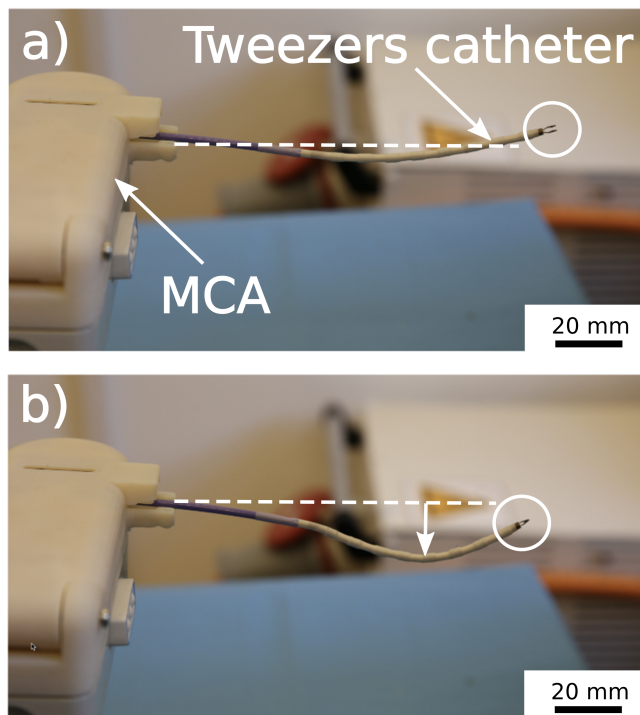


Fig. 4. Influence of the tweezers' pulling wire on a the magnetic catheter in its flexible state. a) Tweezers catheter with open tweezers. b) When the Nitinol wire is pulled to close the tweezers, the flexible body of the catheter bends, moving the tweezers and impeding precise grasping.

was required to fully close the tweezers. In its stiff state, the VS section compensated for the deformation of the catheter body induced by the tension in the Nitinol wire. In order to illustrate the necessity for the VS section, we attempted to close the tweezers with the catheter in its flexible state. Results are depicted in Fig. 4. Without the stabilizing effect of the stiff state, the deformation of the catheter under the pulling force from the Nitinol wire was too large, making it impossible to precisely grasp any object.

At the end of this stage, the tweezers catheter was retracted using the MCA, removed from the trocar and disengaged from the MCA.

C. Covering of the lesion

The patch catheter was advanced using the MCA until the tip of the catheter was positioned over the open lesion. The VS module was then activated to change the state of the VS module from stiff to flexible (Video S3 5s). The catheter carrying the rolled patch was then bent towards the lesion until the patch came into contact with the skin surrounding the lesion. Due to the property of the collagen patch surface, the patch stuck vigorously to the skin on contact (Video S3 5s). The adhesive nature of the patch facilitated its removal from the catheter tip. The patch catheter was then moved in a fan-shape to fully unroll the patch and fully cover the lesion area (Video S3 15s). The patch catheter was then removed through the trocar and MCA. To seal the patch on the fetus' skin, the camera catheter was guided along the edge of the patch using

the Phantom Omni, and the laser was fired in pulses to locally melt the patch edge by pressing the laser pedal (Video S4 20s). As the laser hit and melted the collagen patch, it changed color to show how much of the edge had bonded to the skin. Once the lasing phase was completed, the camera catheter was extracted from the trocar and MCA. Subsequently, both trocars were removed from the abdomen. Sequences of the experimental covering of the lesion are depicted in Fig. 6.

III. DISCUSSION

A. Monopolar cutting

The lower conductivity of the tissue model used in this work required monopolar cutting power one order of magnitude higher than what would be used on a real fetus. This higher power resulted in a wider cutting line and the generation of smoke that could at times reduce the quality of the camera view. We believe that these issues would not be encountered when operating on a real fetus, as the fetus skin and tissue have a higher conductivity than *ex vivo* tissue.

The ability to trigger the cutting function using the external pedal allowed the surgeon to start cutting only when the tool was positioned at the desired location, thus significantly reducing possible risks associated with the cutting tool. We also believe that the control method with the phantom omni would be intuitive to a surgeon allowing for immediate familiarisation with catheter steering.

B. Grasping task

While the tweezers catheter was specifically used to remove the recessed porcine flesh, the tool could also be used for a variety of grasping operations in other types of minimally invasive procedures. The combination of the VS module and magnetic steering allows for high bending angles (up to 90°) of the tweezers catheter tip, making it suitable for grasping or holding a multitude of objects at different positions and angles.

C. Covering task

The patch catheter was inserted with the porcine collagen patch rolled onto the tip. The patch was moistened with water to make it flexible and was rolled tightly onto the catheter tip. As the patch was cut in an elliptical shape, it was important to position the patch catheter such that once the patch was unrolled, the lesion would be fully covered. Subsequent changes in orientation or position proved difficult due to the highly adhesive nature of the patch.

To seal the patch to the porcine flesh, we utilized a 1064 nm fiber laser to locally melt the collagen with the heat generated from the interaction of the laser beam and the collagen patch itself. One of the difficulties that we encountered was to determine the appropriate amount of time and power required by the laser to provide a tight bond with the porcine flesh. To establish the correct parameter, we conducted a series of tests with the collagen patches and the porcine skin. We believe a similar approach could be used in the case of fetal skin, but further tests will be required as the final procedure aims to



Fig. 5. Experimental defect resection. a) Sequence showing the monopolar catheter cutting the porcine flesh disc. In the left column, the experiment is demonstrated by opening one panel of the abdomen model. In the right column, the experiment is demonstrated using only the camera catheter view with the abdomen model completely closed. The catheter was guided in a rectangular pattern using the external magnetic field. For this experiment, the monopolar catheter was set to a cutting power of 150 W. The high power produced a small amount of smoke when the experiment was conducted in the completely closed model. b) The severed porcine flesh rectangle was removed using the tweezers catheter. The catheter was initially in the flexible state. In this state the VS section is flexible and allows the catheter tip to be guided towards the skin to be removed. When the tweezers tip was within grasping range, the VS module was switched to the hard state. After 20 s the VS module was rigid and the Nitinol wire was pulled to close the tweezers and grasp the porcine flesh. The tweezers catheter was then retracted in the trocar.

use a personalized bioengineered patch instead of a collagen one. The collagen patch was used to verify and demonstrate the ability of introducing, placing and fixing a patch using our magnetically guided instrumentation. For future *in vivo* experiments, more in-depth studies will be required to validate this lesion closure method compared to traditional suturing.

IV. CONCLUSION

This work demonstrates for the first time a prenatal magnetically assisted endoscopic procedure for the treatment of

MMC in a remote and minimally invasive manner. For successful translation of the prenatal open surgery to a minimally invasive approach, we proposed a magnetically assisted robotic procedure to replace the large and rigid traditional endoscopes with custom made magnetically guided catheters.

The proposed procedure features access through the patient's abdomen using two 11 Fr- trocars and the use of flexible magnetic catheters, which significantly reduces the impact and risks on the mother undergoing the surgery compared to open surgery or a traditional laparoscopy procedure. More

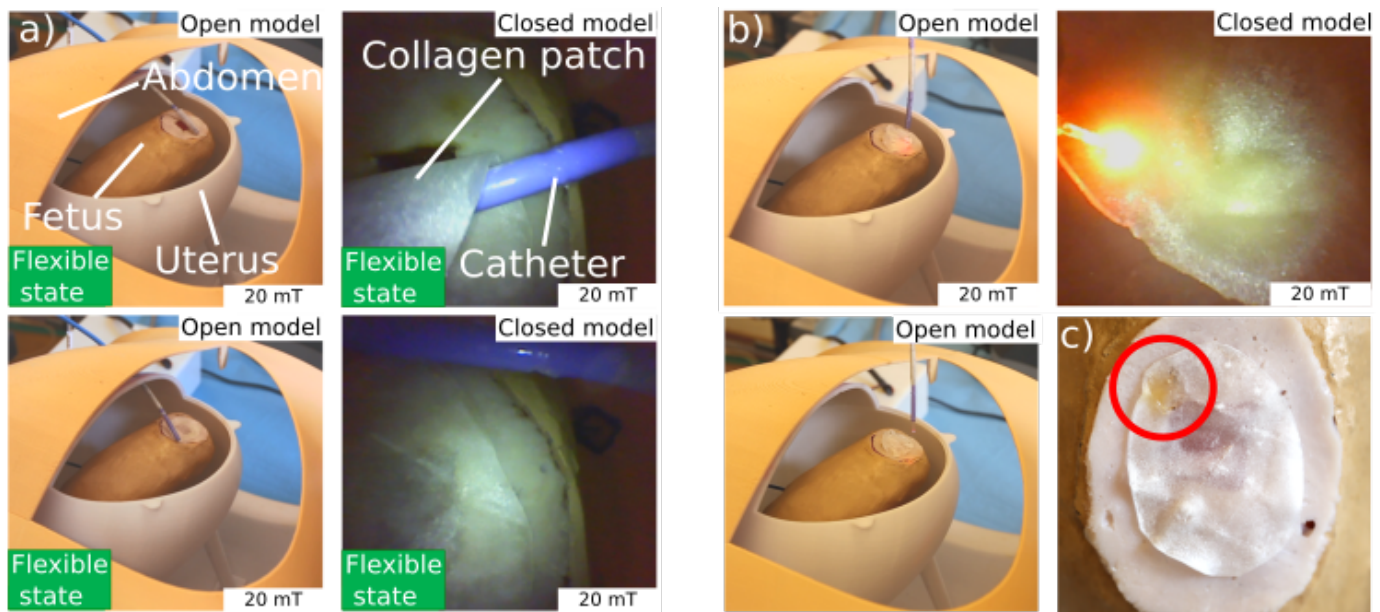


Fig. 6. Experimental covering of the lesion. a) The patch catheter was used to unroll a porcine collagen patch onto the open lesion. The light adhesive nature of the porcine collagen patch helped the patch adhere to the simulated fetus skin. b) The patch was fixed to the fetus skin by locally melting the patch edge using a surgical laser. A 500 μm glass fiber running in a lumen parallel to the working channel of the camera transmitted the beam. The laser was activated using a foot pedal. The melting procedure was conducted in a spot-b-spot manner to ensure equal lasing conditions for the entire edge of the collagen patch. As can be observed in c), the color of the patch changed from pale pink to dark yellow as a consequence of lasing. The dark yellow area was robustly bound to the porcine flesh.

specifically, the reduction of the trocars port size and number alleviate the risk associated with the rigid tools used during a traditional laparoscopy. Additionally the procedure can be conducted in a fully remote manner, which is unique to this robotic approach.

We developed four magnetic endoscopic tools to perform high frequency radio surgery, grasping operations, deployment of collagen patches, and to provide endoscopic video and laser fiber access. These tools have been designed to be compatible with the same trocars and MCA, thus simplifying the transition between the different steps of the surgical operation and reducing the time and risk associated with tool swapping.

An experimental setup was created composed of a female abdomen phantom, a 26th-week-gestation uterus model, and a fetus model. A combination of a tomato flesh disk and porcine flesh was used to simulate the lesion to be repaired.

We successfully demonstrated *in vitro* the three main stages of the procedure using our custom magnetic tools and eMNS, namely 1) the resection of the defect, 2) the removal of the resected sac, and 3) the covering of the lesion using a collagen patch.

Based on the results presented here, we believe that a magnetically assisted robotic surgery of MMC, the most severe form of spina bifida, could be a viable alternative to the more traditional prenatal open surgery approach, with diminished risks for both fetus and mother, while maintaining all the benefits of the traditional prenatal procedure.

ACKNOWLEDGMENT

This work was supported by the Swiss National Science Foundation through grant numbers 200020B_185039, and the

ERC Advanced Grant 743217 Soft Micro Robotics (SOM-BOT). This work has been partially funded by BRIDGE through grant number 180861. We acknowledge partial funding from the European Union's Horizon 2020 research and innovation program under grant agreement 952152.

REFERENCES

- [1] C. E. Eduardo Castilla Vice-Chairperson Lorenzo D Botto, M. K. Bakker, V. Carlo Mirabello, P. Mastroiacovo, and S. Zezza Emanuele Leoncini Priscilla Carcione Lucia Mazzanti, "Annual report 2011 (with data for 2009)," International clearinghouse for birth defects surveillance and research (ICBDSR), Tech. Rep., 2010. [Online]. Available: www.icbdsr.org
- [2] A. J. Copp, N. S. Adzick, L. S. Chitty, J. M. Fletcher, G. N. Holmbeck, and G. M. Shaw, "Spina bifida," *Nature Reviews Disease Primers*, vol. 1, 4 2015.
- [3] M. Meuu, C. Meuli-Simmen, G. M. Hutchins, C. D. Yingling', K. M. Hoffman, M. R. Harrison, and N. S. Adzick, "In utero surgery rescues neurological function at birth in sheep with spina bifida," *NATURE MEDICINE*, vol. 1, no. 4, 1995.
- [4] M. Meuli and U. Moehrlen, "Fetal Surgery for Myelomeningocele: A Critical Appraisal," *European Journal of Pediatric Surgery*, vol. 23, no. 2, pp. 103–109, 2013.
- [5] Lee-Yang, Leonard J. Paulozzi, and C. Wong, "Survival of infants with spina bifida: a population study,1979–94," *Pediatric and perinatal epidemiology*, pp. 374–378, 2001.
- [6] J. P. Bruner, W. O. Richards, N. B. Tulipan, T. L. Arney, and D. Nashville, "Endoscopic coverage of fetal myelomeningocele in utero," *Am J Obstet Gynecol*, pp. 153–158, 1999.
- [7] Pippa Oakeshott1, Gillian M Hunt, Alison Poulton, and Fiona Reid, "Open spina bifida: birth findings predict long-term outcome," *Archives of Disease in Childhood*, vol. 97, pp. 474–476, 2012.
- [8] M J Korenromp, J D van Gool, H W Bruinese, and R Kriek, "Early fetal leg movements in myelomeningocele," *The Lancet*, vol. 327, no. 8486, pp. 917–918, 1986.
- [9] D. A. Sival", J. H. Begeer, A. L. Staal-Schreinemachersb, J. M. E. Vos-Nid, J. R. Beekhuisd, and H. F. R. Prechtl, "Perinatal motor behaviour and neurological outcome in spina bifida aperta," *Early Human Development*, vol. 1, no. 50, pp. 23–37, 11 1997.

- [10] S. Bouchard, M. G. Davey, N. E. Rintoul, D. S. Walsh, L. B. Rorke, N. S. Adzick, D. Farmer, and J. O'Neill, "Correction of hindbrain herniation and anatomy of the vermis after in utero repair of myelomeningocele in sheep," in *Journal of Pediatric Surgery*, vol. 38, no. 3. W.B. Saunders, 3 2003, pp. 451–458.
- [11] B. Martin Meuli, C. Meuli-Simmen, C. D. Yingling, G. M. Hutchins, K. McBiles Hoffman, M. R. Harrison, and N. Scott Adzick San Francisco, "Creation of myelomeningocele in utero: a model of functional damage from spinal cord exposure in fetal sheep," *Journal of Pediatric Surgery*, pp. 1028–1032, 1995.
- [12] H. T. Housley, J. L. Graf, G. S. Lipshultz, C. J. Calvano, M. R. Harrison, D. L. Farmer, and R. W. Jennings, "Creation of Myelomeningocele in the Fetal Rabbit," *Fetal Diagnosis and Therapy*, vol. 15, pp. 275–279, 2000.
- [13] D. A. Pedreira, P. R. Valente, R. C. Abou-Jamra, C. L. Pelarigo, L. M. Silva, and S. Goldenberg, "Successful fetal surgery for the repair of a 'myelomeningocele-like' defect created in the fetal rabbit," *Fetal Diagnosis and Therapy*, vol. 18, no. 3, pp. 201–206, 2003.
- [14] M. P. Johnson, L. N. Sutton, N. Rintoul, T. M. Crombleholme, A. W. Flake, L. J. Howell, H. L. Hedrick, R. D. Wilson, and N. S. Adzick, "Fetal myelomeningocele repair: short-term clinical outcomes." *American journal of obstetrics and gynecology*, vol. 189, no. 2, pp. 482–487, 2003.
- [15] L. Vonzun, M. K. Kahr, F. Noll, L. Mazzone, U. Moehrlen, M. Meuli, M. Hüslér, F. Krähenmann, R. Zimmermann, and N. Ochsenschein-Kölblle, "Systematic classification of maternal and fetal intervention-related complications following open fetal myelomeningocele repair – results from a large prospective cohort," *BJOG: An International Journal of Obstetrics and Gynaecology*, vol. 128, no. 7, pp. 1184–1191, 6 2021.
- [16] M. C. Dewan and J. C. Wellons, "Fetal surgery for spina bifida," *Journal of Neurosurgery: Pediatrics*, vol. 24, no. 2, pp. 105–114, 2019.
- [17] K. Harada, B. Zhang, S. Enosawa, T. Chiba, and M. G. Fujie, "Bending Laser Manipulator for Intrauterine Surgery and Viscoelastic Model of Fetal Rat Tissue," in *IEEE International Conference on Robotics and Automation*. IEEE, 2007.
- [18] Kanako Harada, Kota Tsubouchi, Masakatsu G. Fujie, and Toshio Chiba, "Micro Manipulators for Intrauterine Fetal Surgery in an Open MRI," *International Conference on Robotics and Automation*, 2005.
- [19] T. Vandebroek, M. Ourak, C. Gruijthuisen, A. Javaux, J. Legrand, T. Vercauteren, S. Ourselin, J. Deprest, and E. Vander Poorten, "Macro-Micro Multi-Arm Robot for Single-Port Access Surgery," *International Conference on Intelligent Robots and Systems (IROS)*, 2019.
- [20] R. W. Dobbs, W. R. Halgrimson, S. Talamini, H. T. Vigneswaran, J. O. Wilson, and S. Crivellaro, "Single-port robotic surgery: the next generation of minimally invasive urology," *World Journal of Urology*, vol. 38, no. 4, pp. 897–905, 4 2020.
- [21] H. Kaan and K. Ho, "Endoscopic robotic suturing: The way forward," *Saudi Journal of Gastroenterology*, vol. 25, no. 5, pp. 272–276, 9 2019.
- [22] S. L. Charreyron, Q. Boehler, A. N. Danun, A. Mesot, M. Becker, and B. J. Nelson, "A Magnetically Navigated Microcannula for Subretinal Injections," *IEEE Transactions on Biomedical Engineering*, vol. 68, no. 1, pp. 119–129, 1 2021.
- [23] J. J. Abbott, E. Diller, and A. J. Petruska, "Magnetic Methods in Robotics," *Robotics, and Autonomous Systems*, vol. 19, no. 4, 2019.
- [24] A. Sacco, F. Ushakov, D. Thompson, D. Peebles, P. Pandya, P. De Coppi, R. Wimalasundera, G. Attilakos, A. L. David, and J. Deprest, "Fetal surgery for open spina bifida," *The Obstetrician & Gynaecologist*, vol. 21, no. 4, pp. 271–282, 10 2019.
- [25] A. Alqahtani, A. Albassam, M. Zamakhshary, M. Shoukri, T. Altokhais, A. Aljazairi, A. Alzahim, M. Mallik, and A. Alshehri, "Robot-assisted pediatric surgery: How far can we go?" *World Journal of Surgery*, vol. 34, no. 5, pp. 975–978, 5 2010.
- [26] L. O. Mair, X. Liu, B. Dandamudi, K. Jain, S. Chowdhury, J. Weed, Y. Diaz-Mercado, I. N. Weinberg, and A. Krieger, "MagnetoSuture: Tetherless Manipulation of Suture Needles," *IEEE Transactions on Medical Robotics and Bionics*, vol. 2, no. 2, pp. 206–215, 4 2020.
- [27] S. K. Patel, M. A. Habli, D. N. McKinney, S. M. Tabbah, F. Y. Lim, J. L. Peiro, and C. B. Stevenson, "Fetoscopic Multilayer, Dural Patch Closure Technique for Intrauterine Myelomeningocele Repair: 2-Dimensional Operative Video," *Operative neurosurgery (Hagerstown, Md.)*, vol. 20, no. 2, pp. E131–E132, 1 2021.
- [28] S. Enosawa, T. Tanemoto, K. Harada, A. Ide, K. Tsubouchi, M. Fujie, T. Takezawa, and T. Chiba, "Vitrified collagen sheet, Vitrigel, a novel biophilic sealant for fetal surgery," in *IFMSS*, 2006.
- [29] S. Enosawa, T. Tanemoto, K. Harada, A. Ide, K. Tsubouchi, M. Fujie, T. Takezawa, and T. Chiba, "Vitrified collagen sheet, Vitrigel, a novel biophilic sealant for fetal surgery," in *IFMSS*, 2006.
- [30] A. Dasargyri, E. Reichmann, and U. Moehrlen, "Bio-engineering of fetal cartilage for in utero spina bifida repair," *Pediatric Surgery International*, vol. 36, no. 1, pp. 25–31, 1 2020.
- [31] L. Mazzone, U. Moehrlen, N. Ochsenschein-Kölblle, L. Pontiggia, T. Biedermann, E. Reichmann, and M. Meuli, "Bioengineering and in utero transplantation of fetal skin in the sheep model: A crucial step towards clinical application in human fetal spina bifida repair," *Journal of Tissue Engineering and Regenerative Medicine*, vol. 14, no. 1, pp. 58–65, 1 2020.
- [32] J. Edelmann, A. J. Petruska, and B. J. Nelson, "Magnetic control of continuum devices," *The International Journal of Robotics Research*, vol. 36, no. 1, pp. 68–85, 2017.
- [33] I. Tunay, "Modeling magnetic catheters in external fields." *Conference proceedings : ... Annual International Conference of the IEEE Engineering in Medicine and Biology Society. IEEE Engineering in Medicine and Biology Society. Conference*, vol. 3, pp. 2006–2009, 2004.
- [34] J. Lussi, M. Mattmann, S. Sevim, F. Grigis, C. De Marco, C. Chautems, S. Pané, J. Puigmartí-Luis, Q. Boehler, and B. J. Nelson, "A Submillimeter Continuous Variable Stiffness Catheter for Compliance Control," *Advanced Science*, 2021.
- [35] T. Karacolak, R. Cooper, E. S. Unlu, and E. Topsakal, "Dielectric properties of porcine skin tissue and in vivo testing of implantable antennas using pigs as model animals," *IEEE Antennas and Wireless Propagation Letters*, vol. 11, pp. 1686–1689, 2012.
- [36] Rickie Wade and James Henderson, "Plastic surgery skills course for medical undergraduates," *Journal of Clinical Skills*, 2009.